Molecular Biology of the Cell
Vol. 18, 4591–4602, November 2007

Dual Actin-bundling and Protein Kinase C-binding Activities of Fascin Regulate Carcinoma Cell Migration Downstream of Rac and Contribute to Metastasis[D] [V]

Yosuke Hashimoto,* Maddy Parsons,† and Josephine C. Adams*‡

*Department of Cell Biology, Lerner Research Institute, and ‡Department of Molecular Medicine, Cleveland Clinic Lerner College of Medicine, The Cleveland Clinic, Cleveland, OH 44195; and †Randall Division of Cell and Molecular Biophysics, King's College London, Guy's Campus, London SE1 1UL, United Kingdom

Submitted February 21, 2007; Revised August 29, 2007; Accepted August 31, 2007
Monitoring Editor: Yu-li Wang

Recurrence of carcinomas due to cells that migrate away from the primary tumor is a major problem in cancer treatment. Immunohistochemical analyses of human carcinomas have consistently correlated up-regulation of the actin-bundling protein fascin with a clinically aggressive phenotype and poor prognosis. To understand the functional and mechanistic contributions of fascin, we undertook inducible short hairpin RNA (shRNA) knockdown of fascin in human colon carcinoma cells derived from an aggressive primary tumor. Fascin-depletion led to decreased numbers of filopodia and altered morphology of cell protrusions, decreased Rac-dependent migration on laminin, decreased turnover of focal adhesions, and, in vivo, decreased xenograft tumor development and metastasis. cDNA rescue of fascin shRNA-knockdown cells with wild-type green fluorescent protein-fascin or fascins mutated at the protein kinase C (PKC) phosphorylation site revealed that both the actin-bundling and active PKC-binding activities of fascin are required for the organization of filopodial protrusions, Rac-dependent migration, and tumor metastasis. Thus, fascin contributes to carcinoma migration and metastasis through dual pathways that impact on multiple subcellular structures needed for cell migration.

INTRODUCTION

Carcinomas are the most prevalent form of malignant neoplasm, and they account for the majority of cancer deaths each year. Despite many improvements in early detection and surgical treatment, the recurrence of secondary, metastatic tumors that are resistant to conventional treatments remains a major cause of morbidity and mortality (for review, see Christofori, 2006). Understanding the early events that enable carcinoma cell migration and invasion is thus an important research goal that has potential to improve early diagnosis of aggressive tumors and to stimulate new approaches toward molecularly based adjuvant therapies.

Migration and invasion of carcinoma cells are highly coordinated processes that depend in large part on alterations to cell–cell and cell–extracellular matrix (ECM) adhesion properties and the molecular composition and organization of the actin cytoskeleton (for review, see Guo and Giancotti, 2004; Carragher and Frame, 2004). Direct imaging of carcinoma cell migration in ECM layers and in living primary tumors has revealed that carcinoma cells migrate singly or as collective groups, often undergoing directed movement along collagen fibers. Within the local stroma, this mode of migration involves extensive assembly of cell protrusions, whereas specialized, ECM-degrading adhesions termed invadopodia or podosomes may mediate intravasation (for review, see Friedl and Wolf, 2003; Condeelis *et al*., 2005). Several approaches have identified gene expression profiles that distinguish invading cells from cells that remain within the primary tumor. Micropipet collection of cells chemotaxing toward epidermal growth factor in rat and mouse carcinoma models identified a gene expression signature in which transcripts for multiple actin-binding and regulatory proteins were up-regulated (Wyckoff *et al*., 2000; Condeelis *et al*., 2005). Comparative gene expression profiling of primary and metastatic tumors has begun to address the issue of metastasis to specific organs and to demonstrate significant alterations in the expression of cytoskeletal components (van't Veer *et al*., 2002; Minn *et al*., 2005).

Other candidate markers of migratory carcinoma cells have been identified at protein level by immunohistochemical analyses of clinical specimens. With regard to cytoskeletal reorganizations in carcinoma cells, the actin-bundling protein fascin has emerged as a very interesting candidate biomarker because its expression is low or absent in the majority of normal adult epithelia, yet up-regulation of the protein has been reported in all forms of human carcinoma studied to date. Consistently, irrespective of the tissue source of the tumor, primary carcinomas with high levels of fascin correlate with a clinically aggressive phenotype and poor prognosis (Maitra *et al*., 2002; Pelosi *et al*., 2003; Hashimoto *et al*., 2004, 2005a,b, 2006; Yoder *et al*., 2005; Zigeuner *et al*., 2006). Whether fascin contributes functionally to metastasis

This article was published online ahead of print in *MBC in Press* (http://www.molbiolcell.org/cgi/doi/10.1091/mbc.E07–02–0157) on September 12, 2007.

[D] [V] The online version of this article contains supplemental material at *MBC Online* (http://www.molbiolcell.org).

Address correspondence to: Josephine C. Adams (adamsj@ccf.org).

Abbreviations used: BIM, bisindolylmaleimide I; IKD, inducible knockdown; LN, laminin; mRFP, monomer red fluorescent protein; shRNA, short hairpin RNA; TetR, tetracycline repressor.

Table 1. Antibodies used in this study

	Monoclonal/polyclonal	Clone	Company/reference
Antibody to			
α-Actinin	Mouse monoclonal	BM-75.2	Sigma (St. Louis, MO)
β-Actin	Mouse monoclonal	AC-15	Sigma
β-Catenin	Mouse monoclonal	14	BD Biosciences
E-cadherin	Mouse monoclonal	36	BD Biosciences
Fascin	Mouse monoclonal	55k2	Dako North America (Carpinteria, CA)
Fascin	Rabbit polyclonal	FAS-C	Adams *et al.* (1999)
GFP	Mouse monoclonal	7.1/13.1	Roche (Indianapolis, IN)
Integrin α2	Mouse monoclonal	HAS-3	Tenchini *et al.* (1993)
Integrin α3	Mouse monoclonal	PIB5	Telios Pharmaceutical (San Diego, CA)
Integrin α5	Mouse monoclonal	Mab11	Akiyama *et al.* (1989)
Integrin α6	Rat monoclonal	135-13C	Costantini *et al.* (1990)
Integrin β1	Mouse monoclonal	K20	Staquet *et al.* (1989)
Paxillin	Mouse monoclonal	349	BD Biosciences
Phosphotyrosine	mouse monoclonal	4G10	Upstate (Millipore)
Rac 1	Mouse monoclonal		Chemicon International (Temecula, CA)
Tet repressor	Rabbit polyclonal		MoBiTec (Göttingen, Germany)
Vinculin	Mouse monoclonal	VIN-11-5	Sigma
Anti-mouse AP	Goat		Tropix (Bedford, MA)
Anti-rabbit AP	Goat		Tropix
Anti-mouse FITC	Goat		MP Biomedicals (Solon, OH)
Anti-rat FITC	Goat		Sigma
Anti-mouse Alexa Fluor 568	Goat		Invitrogen
Reagents/chemicals/antibiotics			
Phalloidin	Rhodamine conjugated		Invitrogen
BIM			Calbiochem
NSC23766			Calbiochem
Y27362			Calbiochem
Blasticidin			Invitrogen
Doxycycline			Sigma
G-418			Sigma
Puromycin			BD Biosciences

is largely unknown; however, high fascin protein in the primary carcinoma has been correlated with local lymph node or distant metastases (Hashimoto *et al*., 2004; Puppa *et al*., 2007) or with an increased frequency of metastastic disease (Zigeuner *et al*., 2006). The fascin transcript is a component of a gene signature that correlates with breast cancer metastasis to the lung (Minn *et al*., 2005).

To date, the cellular and molecular properties of fascin have been mostly studied in normal mesenchymal and neuronal cells. In vitro, fascin cross-links filamentous actin (F-actin) into tightly packed, parallel bundles in cooperation with Arp2/3 complex and Wiskott-Aldrich syndrome protein (Vignjevic *et al*., 2003; Haviv *et al*., 2006). In intact cells, fascin-and-actin bundles support cortical cell protrusions and growth cone filopodia (Yamashiro *et al*., 1998; Adams *et al*., 1999; Cohan et al., 2001, Adams and Schwartz, 2000; Anilkumar *et al*., 2003; Svitkina *et al*., 2003; Vignjevic *et al*., 2006). Fascin contains N- and C-terminal actin-binding sites and the actin cross-linking activity of fascin is negatively regulated by a protein kinase C (PKC) phosphorylation site (serine-39 in human fascin) that lies within the amino-terminal actin-binding site (Ono *et al*., 1997). The balance between nonphosphorylated and phosphorylated fascin in cells is governed by ECM components and other extracellular cues (for review, see Adams, 2004). The expression of fascin in carcinoma cells represents an aberrant situation for which the regulatory mechanisms and specific functional consequences are largely unknown (for review, see Hashimoto *et al*., 2005a). Fascin overexpression or depletion were reported to result in altered carcinoma cell migration, but the mechanisms of how fascin affects this endpoint remain unclear (Jawhari *et al*., 2003; Hashimoto *et al*., 2005b; Xie *et al*., 2005). Here, we have developed inducible knockdown of fascin in human colon carcinoma cells to establish the functional contribution of fascin in carcinoma cells and in vivo.

MATERIALS AND METHODS

Cell Lines and Other Materials

SW480, SW1222, and DLD-1 human colon cancer cell lines were cultured in DMEM plus 10% fetal calf serum (FCS). C2C12 mouse skeletal myoblasts were grown in DMEM plus 20% FCS. All cells were maintained at 37°C in a humidified 5% CO_2 atmosphere. All antibodies, antibiotics and pharmacological reagents are listed in Table 1. GFP-fascin plasmids for *Homo sapiens* fascin-1 were as described previously (Adams *et al*., 1999; Adams and Schwartz, 2000). A GFP-*Xenopus tropicalis* fascin-1 expression plasmid was prepared by subcloning *X. tropicalis* fascin-1 cDNA (clone Thda 017B16; obtained from Cambridge University and The Wellcome Trust Sanger Institute and Wellcome Trust/Cancer Research UK Institute *X. tropicalis* EST project; Gilchrist *et al*., 2004) into pEGFP-C (Clontech, Mountain View, CA) by using the polymerase chain reaction (PCR) primers listed in Table 2. The cDNA clone was sequenced in it entirety, and it is deposited as GenBank DQ374150. S33A and S33D mutations of *X. tropicalis* fascin-1 were prepared by PCR-based mutagenesis of green fluorescent protein (GFP)-*Xt*fascin, by using the oligonucleotides listed in Table 2 and the QuikChange II site-directed mutagenesis kit (Stratagene, La Jolla, CA).

Development of SW480 Cells for Inducible Knockdown of Fascin

SW480 cells were transfected with pcDNA6/TR (Invitrogen, Carlsbad, CA) by the PolyFect (QIAGEN, Valencia, CA) method, selected in 10 μg/ml blasticidin, and antibiotic-resistant clones were isolated by ring cloning. Tetracycline repressor (TetR) expression was examined by Western blot. Two clones, with strongest expression, were chosen for further study, and they were transfected with pSUPERIOR vector encoding a short hairpin RNA (shRNA) for human fascin (gift of Yutaka Shimada, Kyoto University). Clones were iso-

Table 2. Oligonucleotide primers used in this study

Primer	Sequence(5′–3′)
Sequence primer for *X. tropicalis* FSCN1	AAGTGGAACCATGAAGGC
Sequence primer for *X. tropicalis* FSCN1	TGATGGTGCTTACAGCCT
Xt-fascin forward for N-terminal GFP tag (Xho I site)	GATCCTCGAGCATGACTTCTGGACCCCTT
Xt-fascin reverse for N-terminal GFP tag (STOP codon + BamHI site)	GATCGGATCCTTAGTATTCCCAGAGTGT
S->A in Xt-fascin forward	GCTTCGGCAAGCGCTTTAAAGAAAAAGCAAGTGTGG
S->A in Xt-fascin reverse	CCACACTTGCTTTTTCTTTAAAGCGCTTGCCGAAGC
S->D in Xt-fascin forward	GCTTCGGCAAGCGATTTAAAGAAAAAGCAAGTGTGG
S->D in Xt-fascin reverse	CCACACTTGCTTTTTCTTTAAATCGCTTGCCGAAGC

List of oligonucleotide primers used in these experiments. All oligonucleotides were synthesized by Sigma-Genosys (The Woodlands, TX).

lated by selection in 1 μg/ml puromycin (BD Biosciences, San Jose, CA) and ring cloning. Conditions for knockdown of fascin were established by doxycycline treatment (0.1–10 μg/ml) for 0–72 h. Expression of fascin in each clone was analyzed by Western blots in triplicate. Cells reexpressing GFP-*Xt*fascin or point mutants were established by transfection and selection in 1 mg/ml Geneticin (G-418; Sigma) for 2 wk. GFP-expressing cells were isolated by cell sorting in a FACSVantage (BD Biosciences), with fluorescent excitation with an Argon laser (excitation at 488 nm). A marker was set 1–2% above the maximum fluorescence of SW480-Pa cells, and cells with fluorescence above this level were collected.

Flow Cytometry

Cells were trypsinized and resuspended at 2×10^7 cells/ml in phosphate-buffered saline (PBS). Then, they were incubated on ice with antibodies to integrin subunits (Table 1) at established appropriate dilutions, or isotype-matched controls, washed, incubated for 30 min with fluorescein isothiocyanate (FITC)-conjugated secondary antibodies, and washed again. Cells were passed through a BD Biosciences FACScan using FlowJo software (Tree Star, Ashland, OR) with fluorescent excitation with an Argon laser (excitation at 488 nm). Ten thousand events were acquired per sample.

Soft Agar Growth Assay

We seeded 35-mm dishes in triplicate with 5×10^2, 5×10^3, or 5×10^4 cells in 1 ml of DMEM containing 10% FCS and 0.35% Noble agar (BD Biosciences) over a base of DMEM containing 10% FCS and 0.5% Noble agar. Dishes were refed with 1 ml of DMEM containing 10% FCS and 0.35% Noble agar each week. Colony formation was scored by microscopical examination after 4 wk.

Tumor Xenografts in Nude Mice

Experiments were carried out by Cleveland Clinic Foundation (CCF) Animal Tumor Core in accordance with institutional guidelines. For subcutaneous injection, eight 5-wk-old female NCr athymic nude (*nu/nu*) mice were injected in the right and left flanks with 10^6 SW480-Pa cells or IKD-F11 cells in 50 μl of PBS, respectively. Mice were randomly assigned into two groups of four. One group received doxycycline ad libitum at 2 mg/ml in the drinking water. Mice were inspected every 3–4 d and tumors measured with calipers over a 32-d period. Volumes were calculated using the formula for a prolate spheroid: $(4/3)\pi ab^2$ (a is major axis and b is minor axis of the tumor). For metastasis experiments, groups of 12 mice were injected intrasplenically with either 5×10^6 SW480-Pa or IKD-F11 cells in 50 μl of PBS. Mice in each group were randomly assigned into two sets of six. One set of each cell line received doxycycline as described above. In total, six mice were removed from the experiment because they died the day after inoculation. Other mice were inspected every 3–4 d for 7 wk. For analysis of metastatic behavior of GFP-*Xt*fascin subclones, groups of six mice were injected intrasplenically with 2×10^6 IKD-F11 cells stably expressing either GFP, GFP-*Xt*fascin, GFP-*Xt*fascinS33A, or GFP-*Xt*fascinS33D, in 50 μl of PBS. All mice were maintained on doxycycline and inspected every 3–4 d for 8 wk. At the end of each experiment, all mice were killed by CO_2 inhalation and necropsied. Primary spleen tumors and macroscopic metastatic tumors in the abdomen, liver, or ovary were recorded. Tumors were resected and either fixed in 10% formaldehyde/PBS or snap-frozen in liquid nitrogen and stored at −80°C for immunoblotting. Fixed tumors were paraffin-embedded, sectioned, and stained with hematoxylin and eosin or immunostained for human fascin as described previously (Yoder *et al.*, 2005).

Scanning Electron Microscopy

Cells plated on 15 nM laminin (LN) for 2 h were fixed in 1.6% paraformaldehye/2.5% glutaraldehyde and postfixed with 1% osmium tetroxide and 0.5% uranyl acetate. Samples were dehydrated through a series of graded ethyl alcohols (70–100%), followed by chemical drying in hexamethyldisilazane. Cells were coated with gold and examined under a JEOL JSM-5310 microscope by using JUS DSG1 Digital Imaging Console version 2.30C (JEOL USA, Peabody, MA).

Fluorescence Microscopy

Experiments were carried out with cells plated for 2 h on 15 nM LN; in some experiments, cells were pretreated with inhibitors. Indirect immunofluorescent stainings for fascin, α-actinin, phosphotyrosine, and vinculin were carried out as described previously (Adams, 1997; Anilkumar *et al.*, 2003). Samples labeled with FITC, tetramethylrhodamine B isothiocyanate, or Alexa 568 fluorochromes were examined at room temperature under a Leica DM RXE(TCS-SP/SP-AOSB) confocal laser scanning microscope with HCX Plan Apo 63× numerical aperture 1.4 oil immersion objective lens, using Leica confocal software version 2.5 (Leica, Wetzler, Germany). Confocal images were acquired as Z stacks or single XY sections at room temperature. In some experiments, projections of image stacks were prepared in Volocity version 3.7.0 (Improvision, Coventry, United Kingdom).

Transfilter Migration Assay

We seeded 2.5×10^4 cells/well into the top chambers of a 24-well, 8-μm pore-size micropore polycarbonate membrane filter (BD Biosciences), and the lower chambers were filled with DMEM containing 10% FCS as a chemoattractant and incubated for 24 h at 37°C. Cells remaining on the upper surface were carefully removed with a cotton swab, and the membranes were fixed and stained with Diff-Quik stain (Dade Behring, Deerfield, IL). Migration was quantified by counting the migrated cells in five random 20× magnification fields per filter. At least three independent experiments were carried out.

Time-Lapse Imaging of Migrating Cells

Cells were plated for 1 h at 37°C in serum-free DMEM on glass-bottomed dishes (MatTek, Ashland, MA) coated with 15 nM LN and blocked with 1 mg/ml heat-denatured bovine serum albumin. Pilot experiments established this concentration to be optimal for haptokinetic (i.e., random migration on uniform ECM) cell migration. Nonattached cells were rinsed off, and the remaining cells, in serum-free DMEM, were placed into a temperature- and CO_2-controlled incubator (at 37°C, 5% CO_2) on the stage of a Leica DMIRE2 inverted microscope (Leica), equipped with electronically controlled shutters and filter wheel. Phase contrast images were captured under a 20× objective with a camera controller C4742_95 (Hamamatsu, Bridgewater, NJ), run by Improvision Openlab software, version 3.1.5, every 4 min for 50 frames (in total, 200 min). In some experiments, cells were pre-treated with pharmacological agents as described in the text. All reagents were maintained throughout the experiments at the same concentrations as used for pretreatment. Mean cell speed (defined as length of the migration trajectory divided by time) and net migration (defined as straight-line distance between the starting and ending points) were calculated from traces of the displacement of each cell centroid prepared in Improvision Openlab 3.1.5 and analyzed in Excel (Microsoft, Redmond, WA). At least three independent experiments were carried out for each experimental condition.

Analysis of Focal Adhesion Disassembly

Cells were transfected with monomeric red fluorescent protein (mRFP)-paxillin (gift of Martin Humphries, University of Manchester, Manchester, United Kingdom) and 36 h later plated onto glass-bottom dishes coated with 15 nM LN. After 2 h of adhesion, cells were imaged using a CARV spinning disk head attached to a Leica DMIRB widefield microscope. All images were acquired using a 40×/1.3 oil immersion objective at 37°C. Images were acquired using separate Cy3 excitation and emission filter sets (Ludl, Hawthorne, NY) controlled by automatic excitation and emission wheels (Ludl) on an Orca ER charge-coupled device camera (Hammamatsu). Acquisition was performed using Andor IQ software (Andor, Belfast, Northern Ireland).

Frames were acquired every 20 s over 20 min. Analysis of focal adhesion disassembly kinetics was performed in NIH ImageJ (http://rsb.info.nih.gov/ij/index.html). A background correction mask was applied to all frames within a single movie to highlight the RFP-positive structures. Adhesions either present at the beginning of filming period, or appearing during filming, were manually tracked through the entire time-lapse series until the time when they dissolved, i.e., when fluorescence intensity was no longer visible. The percentage of all adhesions that dissolved over time was calculated from tracking 12 cells in each population in three independent experiments. The mean time taken for adhesions to disappear in each cell line, in the absence or presence of doxycycline, was calculated from measuring the time to dissolution for adhesions from multiple cells. For each cell line, measurements were taken from 12 to 15 adhesions from five cells from three independent experiments.

Rac Activity Assay

Rac-GTP was quantified using the G-LISA Rac activation assay kit according to manufacturer's procedure (Cytoskeleton, Denver, CO). Lysates were prepared from IKD-F11 Fas+ and Fas− cells plated on 15 nM LN for 2 h, and from IKD-F11 Fas+ cells treated with 100 μM NSC23766 overnight. C2C12 cells in suspension or plated on 50 nM fibronectin (FN) for 15 min were used as controls for the method (Adams and Schwartz, 2000). Experiments were done in triplicate.

Gel Electrophoresis and Immunoblotting

Whole cell lysates were prepared in SDS-polyacrylamide gel electrophoresis sample buffer buffer (2% SDS, 10% glycerol, and 50 mM Tris-HCl, pH 6.8). Tumor extracts were prepared from frozen samples that were powdered with a pestle and mortar in liquid nitrogen, extracted in radioimmunoprecipitation assay buffer containing protease inhibitor cocktail, sonicated, and centrifuged. All samples were electrophoresed on 10% or 12.5% polyacrylamide gels under reducing conditions and transferred to polyvinylidene difluoride membranes (Millipore, Billerica, MA) by using a semidry transfer blot system. After blocking with Tris-buffered saline containing 1% Tween 20, 2% skim milk, and 0.5% bovine serum albumin for 1 h, the membranes were incubated with the primary antibodies (Table 1) and developed with alkaline phosphatase-conjugated secondary antibodies (Table 1) and enhanced chemiluminescence as described previously (Anilkumar *et al*., 2003). Quantitative analysis was performed using NIH ImageJ, version 1.38.

RESULTS

Setup of Inducible Fascin-Knockdown Human Colon Carcinoma Cells

We selected SW480 cells, a well-established model of colon carcinoma cells that derive from an aggressive primary human colonic adenocarcinoma (Kyriazis *et al*., 1978), and that have high endogenous fascin (Figure 1A), as suitable for fascin-knockdown experiments. To enable inducible knockdown of fascin transcripts, clonal derivatives of SW480 with stable expression of the TetR protein were developed (designated "parental", Pa or PaA; Figure 1B). Stable transfection of these lines with pSUPERIOR plasmid then provided tetracycline-inducible expression of a previously validated shRNA against human fascin-1 (Hashimoto *et al*., 2005b). Individual clones were tested for continued expression of fascin in the absence of the shRNA (Fascin+ condition) or with doxycycline induction of shRNA expression (Fascin−

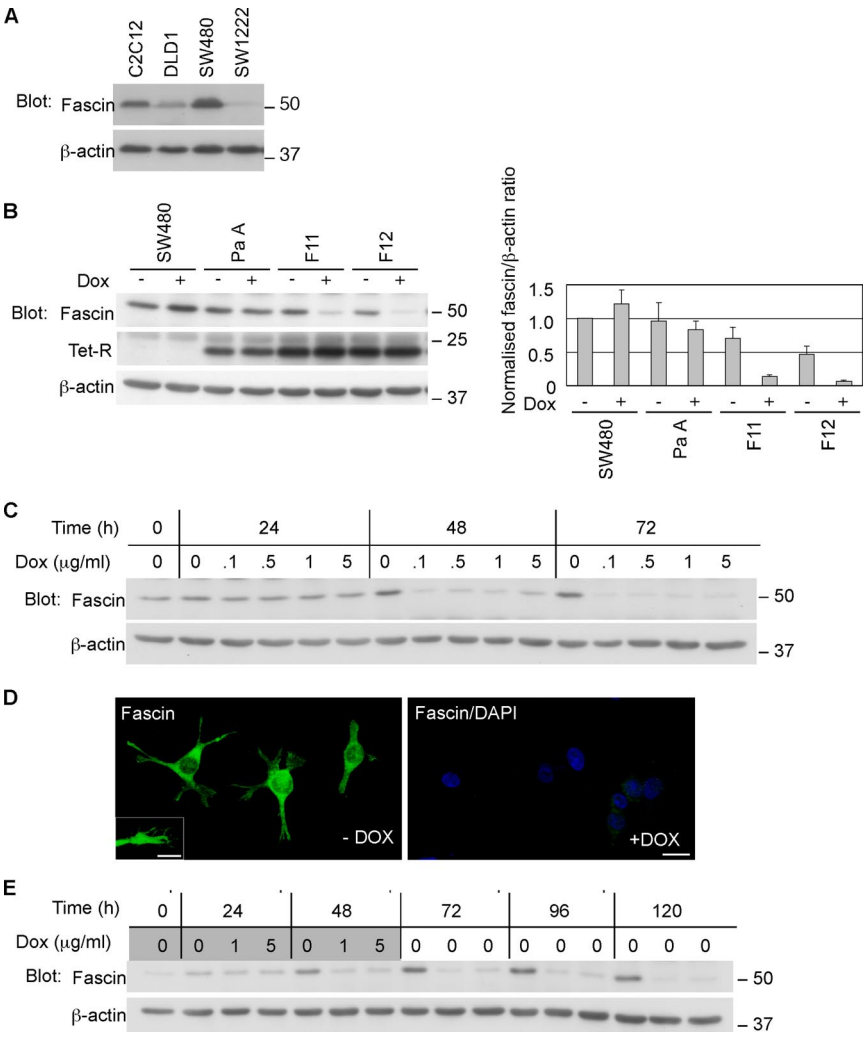

Figure 1. Development of inducible fascin-knockdown SW480 cells. (A) Immunoblot for fascin expression in human colon carcinoma cell lines. C2C12 skeletal myoblasts were used as a normal cell control. (B) Development of SW480 cells expressing TetR (PaA) and inducible fascin-knockdown clones F11 and F12. Doxycycline was applied at 1 μg/ml for 72 h. Graph shows normalized fascin levels (±SD) by scanning densitometry from triplicate experiments. (C) Time and concentration dependence of fascin knockdown in IKD-F11 cells. (D) Indirect immunofluorescent staining for fascin, in IKD-F11 cells maintained in the absence or presence of 0.5 μg/ml doxycycline for 72 h. Bar, 20 μm. Inset, detail of fascin-containing protrusions and associated filopodia. Bar, 10 μm. (E) Persistence of fascin knockdown. IKD-F11 cells were left untreated as controls or treated with the indicated concentrations of doxycycline for 48 h (shaded doxycycline panel), and then they were cultured in the absence of doxycycline for 72 h (unshaded, no doxycycline). The total experimental time was 120 h. Replicate cultures were lysed at the indicated timepoints and the levels of fascin protein examined by immunoblot during and after doxycycline treatment. Fascin knockdown in samples that had received doxycycline persisted for 72 h. Molecular mass markers are in kilodaltons.

condition). Whereas SW480 and SW480-PaA cells maintained the same level of fascin protein irrespective of the addition of doxycycline, the inducible knockdown (IKD) subclones showed substantial and specific reduction of fascin. Several IKD subclones with >80% knockdown of fascin in the presence of doxycycline were chosen for further experiments (IKD-F11 and IKD-F12 in Figure 1B). Treatment with 0.1 μg/ml doxycycline for 48 h was sufficient to decrease fascin levels by 90% in IKD-F11 cells (Figure 1C). Inspection by indirect immunofluorescent staining for fascin demonstrated that fascin was present in the cell bodies, protrusions, and filopodial tips of IKD-F11 Fas+ cells and that the level of knockdown in IKD-F11 Fas− cells was uniform across the cell population (Figure 1D). After application of 1 μg/ml doxycycline for 48 h, knockdown of fascin was maintained for at least 120 h (Figure 1E).

Fascin Knockdown Leads to Altered Morphology of Cell Protrusions

On fascin depletion, the morphology of IKD subclones as colonies in standard tissue culture was grossly similar to that of SW480 or SW480-Pa cells. After plating as single cells on LN, a physiologically relevant ECM component to which SW480 cells attach strongly, all cell populations contained a mixture of elongated, spindly cells with multiple finger-like processes and rounded cells (Figure 2A). However, inspection of LN-adherent cells by scanning electron microscopy revealed significant differences in the morphology of the protrusive tips of fascin-depleted cells. IKD-F11 Fas+ cells formed elaborate protrusions that contained multilobed lamellipodia with fine filopodia extending from their edges (Figure 2B). These protrusions were indistinguishable from those of SW480 and SW480-Pa cells. In contrast, IKD-F11 Fas− cells had thinner and less complex protrusions, with loss of the lobed lamellipodia (Figure 2C). These differences were reproducible in multiple IKD clones, and, in terms of F-actin organization, they were apparent as decreased numbers of filopodia and a less concentrated F-actin meshwork at cell edges in the IKD-F11 Fas− cells (Figure 2D). Quantitative scoring demonstrated that the number of filopodia/cell was significantly reduced upon fascin knockdown (Figure 2E; the mean number of filopodia decreased from 24.6 ± 1.6/cell to 12.9 ± 1.1/cell; significant at $p < 0.0001$). Doxycycline treatment of SW480 or SW480-Pa cells did not result in changes to cell protrusions or filopodia (Figure 2A; data not shown). Given that IKD-F12 cells in the absence of doxycycline showed some reduction in the level of fascin (Figure 1B), but no morphological alterations, the results also demonstrate that substantial (>80%) depletion of fascin is needed to produce a phenotypic alteration.

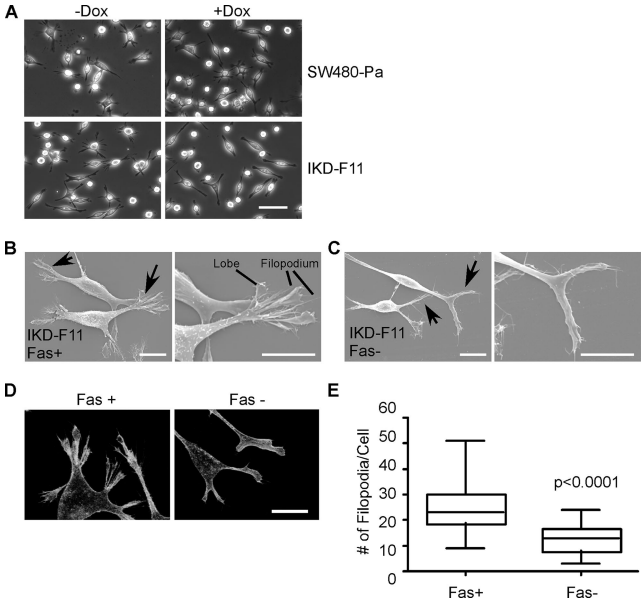

Figure 2. Altered morphology of protrusions and loss of filopodia in fascin-knockdown cells. (A) Phase contrast views of SW480-Pa and IKD-F11 cells after 48 h culture in the absence or presence of 0.5 μg/ml doxycycline and plating for 2 h on 15 nM LN. Bar, 50 μm. (B) Scanning electron micrographs of IKD-F11 Fas+ cells adherent on LN. Examples of protrusions are arrowed (left), with enlarged view of the protrusive tips (right). Bars, 10 μm. (C) Scanning electron micrographs of IKD-F11 Fas− cells adherent on LN. Examples of residual protrusions are arrowed (left), with enlarged view of the tips (right). Bars, 10 μm. (D) F-actin organization in IKD-F11 cells adherent on LN under Fas+ and Fas− conditions. Bar, 20 μm. (E) IKD-F11 Fas− cells have decreased numbers of filopodia. Box and whisker plot of the number of filopodia per cell, quantified from at least 26 phalloidin-stained cells in three independent experiments.

Fascin Knockdown Leads to Reduced Migration and Disassembly of Focal Adhesions

With regard to the mechanisms underlying the changes in cell protrusion morphology, we first considered that cell attachment to the extracellular environment was altered. However, attachment of IKD-F11 Fas− cells to 50 nM fibronectin, laminin, collagen IV, or collagen I, as measured by a previously described cell attachment method (Anilkumar *et al*., 2002), and direct counting of attached cells was not altered relative to IKD-F11 Fas+ cells or SW480 cells (data not shown). SW480 cells express multiple β1 integrins and neither the cell-surface expression of integrin β1, α2, α3, or α6 subunits, nor the levels of β-catenin and E-cadherin were changed upon fascin depletion (data not shown). Some, but not all, clinical studies have correlated fascin expression with the proliferative status of carcinomas (for review, see Hashimoto *et al*., 2005a). However, in soft agar growth assays, IKD-F11 and IKD-F12 Fas− cells proliferated indistinguishably from their Fas+ counterparts and SW480-Pa cells (Supplemental Table 1). Previously, fascin overexpression in fascin-negative SW1222 colon carcinoma cells was reported to increase cell proliferation. However, this result was obtained in a different experimental system of three-dimensional collagen gels that promote integrin-mediated glandular differentiation: these gels do not provide conditions for anchorage-independent growth (Jawhari *et al*., 2003). Because a major role of cell protrusions and filopodia is in cell migration, our subsequent analyses focused on cell migration properties.

IKD-F11 Fas− cells had reduced transfilter migration activity (Figure 3A). Time-lapse imaging also revealed a significant decrease in haptokinetic migration on LN, both in terms of mean speed and the net migration (Figure 3, B and C). Migration of SW480-Pa cells was not altered in the absence or presence of doxycycline (data not shown). The mode of migration of Fas+ cells was complex in all lines, with cells becoming extended and spindly through extension of dynamic protrusions with filopodia and elongation of the tail region, followed by rapid rounding due to tail retraction, and then extension of new filopodia and protrusions in the direction of migration (Supplemental Movie 1). In contrast, Fas− cells either extended without release of the tail region, or extended and then retracted at the front edge, followed by extension at another point on the cell surface,

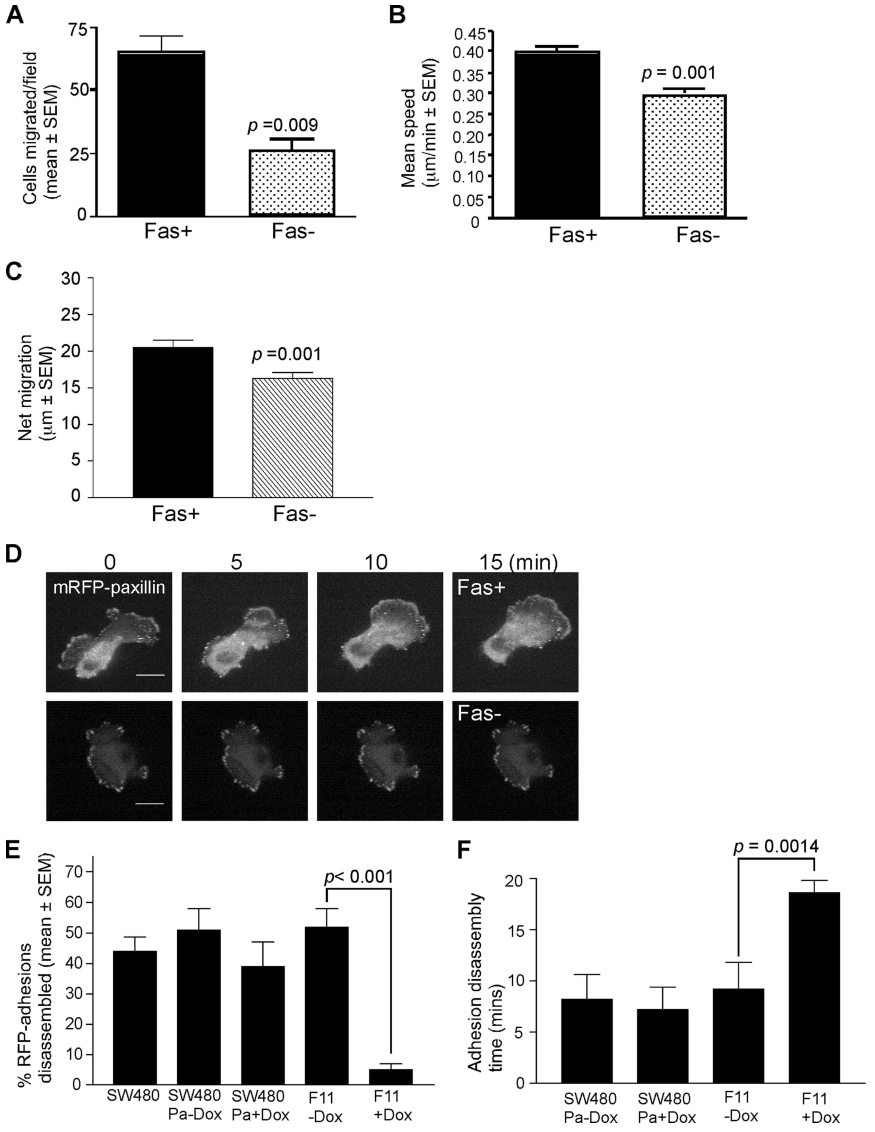

Figure 3. Fascin knockdown decreases cell migration and focal adhesion turnover. (A) transfilter migration of IKD-F11 Fas+ and Fas− cells. Each column is the mean of triplicate experiments; bars indicate SEM. (B) Haptokinetic migration of IKD cells on 15 nM LN. Migration speeds were calculated from time-lapse movies by measurements of the change in position of cell nuclei over time. Each column is the mean of three experiments; bars indicate SEM. See also Supplemental Movies 1 and 2. (C) Directional persistence of IKD cells migrating on LN. Net displacement of cell bodies was calculated from time-lapse movies in the Openlab program. Each column is the mean of three experiments; bars indicate SEM. (D) IKD-F11 cells under Fas+ and Fas− conditions and transiently expressing mRFP-paxillin were plated on 15 nM LN for 4 h. mRFP-paxillin–containing focal adhesions were imaged using a CARV spinning disk microscope by time-lapse imaging. Still images from each time-lapse series are shown at selected time points. Bars, 10 μm. See also Supplemental Movies 3 and 4. (E) Percentage of total adhesions disassembled over time by SW480 and F11 cells under the indicated conditions was calculated in ImageJ. Each column represents mean data from four cells per treatment and three independent experiments; bars indicate SEM. (F) The mean time taken for adhesions to disappear in SW480Pa and IKD-F11 cells, either in the absence or presence of doxycycline, was calculated from measuring 12–15 adhesions from five cells from three independent experiments. Each column represents the mean; bars indicate SEM.

such that the net displacement of cell bodies was decreased (Figure 3C and Supplemental Movie 2).

To examine molecular changes associated with these alterations in cell protrusions and migration, IKD-F11 cells on LN were stained for several components of the actin cytoskeleton and cell adhesions, either under control conditions or with fascin knockdown. The distributions of α-actinin in the cell body cytoskeleton or vinculin in focal adhesions were not obviously altered (Supplemental Figure 1A). In contrast, the ventral surfaces of IKD-F11 Fas− cells contained denser areas of phosphotyrosine-containing adhesions (Supplemental Figure 1A). Immunoblotting of the profile of phosphotyrosine-containing proteins in LN-adherent SW480-Pa, IKD-F11, and IKD-F12 cells established that, in each line, the content of phosphotyrosine-containing proteins was unchanged in the absence or presence of doxycycline (Supplemental Figure 1B). Whereas levels of α-actinin and vinculin were not altered in fascin IKD clones compared with SW480-Pa cells, the phosphotyrosine-containing protein paxillin was consistently elevated (Supplemental Figure 1C). However, paxillin levels were not altered in any cells upon fascin depletion (Supplemental Figure 1C), and we did not observe definite alterations in the paxillin staining of focal adhesions (data not shown). We conclude that the observed alterations in patterning of phosphotyrosine-containing adhesions under Fas− conditions relate to protein relocalization rather than a change in the abundance of phosphotyrosine-containing proteins.

Focal adhesions are transient structures that dynamically assemble and disassemble as cells migrate (Webb *et al.*, 2003). To directly measure kinetic aspects of focal adhesions under control and fascin-depleted conditions, IKD-F11 cells maintained in the presence or absence of doxycycline were transfected with mRFP-paxillin. Cells were plated onto LN, and paxillin-containing focal adhesions were analyzed by fluorescence time-lapse microscopy (Figure 3D). IKD-F11 Fas− cells showed a significant reduction in focal adhesion disassembly. Only 5 ± 2% of the total focal adhesions per cell were disassembled during the 20-min filming period, compared with 52 ± 6% disassembled in Fas+ counterparts (Figure 3E and Supplemental Movies 3 and 4). This change in behavior was specific to fascin-depleted cells because SW480 and SW480Pa cells, which had lower endogenous paxillin than F11 cells, had near-identical percentages of focal adhesions disassembled to IKD-F11 Fas+ cells. Furthermore, the percentage of focal adhesions disassembling

in SW480Pa cells was not significantly altered in the presence of doxycycline (Figure 3E). To measure rates of disassembly, the mean time taken for adhesions to disappear in each cell line, in the absence or presence of doxycycline, was calculated from measuring the time to dissolution for a number of adhesions from multiple cells. The mean time to dissolution was not significantly different between SW480Pa cells, in the absence or presence of doxycycline, or IKD-F11 Fas+ cells. However, it was significantly longer (mean of 18. 6 min vs. 9.2 min) in IKD-F11 Fas− cells (Figure 3F). These data identify a role for fascin in the control of focal adhesion disassembly dynamics.

Fascin Functions in a Rac-dependent Pathway in Colon Carcinoma Cell Migration

To gain insight into the molecular pathways by which fascin participates in carcinoma cell migration, we tested the effects of pharmacological inhibitors of signaling molecules that have generally significant roles in cytoskeletal reorganisations during cell migration. We reasoned that fascin-depleted cells would respond differently to inhibition of mediators that function upstream of fascin. Treatment of cells with bisindolylmalemide I (BIM), an inhibitor of conventional PKC isoforms, or Y27632, an inhibitor of Rho kinase, significantly inhibited migration speed to a similar extent in both IKD-F11 Fas+ and Fas− cells (Figure 4A). In contrast, the Rac inhibitor NSC23766 (Gao *et al*., 2004), significantly decreased the migration of IKD-F11 Fas+ cells yet did not inhibit migration of IKD-F11 Fas− cells (Figure 4A and Supplemental Movies 5 and 6). The migration of NSC23766-treated IKD-F11 Fas− cells was not significantly different from that of NSC23766-treated IKD-F11 Fas+ cells (Figure 4A, lane 4 vs. 8).

We therefore analyzed the status of Rac in LN-adherent Fas+ and Fas− cells. Levels of Rac1 protein were equivalent in parental, IKD-F11 and F12 cells, in the absence or presence of doxycycline (Figure 4B). In the Rac activity assay, C2C12 cells on fibronectin were included as a positive control (Adams and Schwartz, 2000). Levels of Rac-GTP were equivalent in LN-adherent IKF-F11 Fas+ and Fas− cells. As expected, cells treated with NSC23766 had lower Rac activity (Figure 4C). Thus, the Rac independence of migration of IKD-F11 Fas− cells is not due to reduced levels of either Rac protein or Rac activity.

The Actin-bundling and PKC-binding Activities of Fascin Both Contribute to Its Role in Rac-dependent Carcinoma Cell Migration

To establish whether the known actin-bundling and active PKC-binding activities of fascin both contribute to its role in carcinoma cell protrusions and migration, we set up cDNA rescue expression of fascin with *X. tropicalis* fascin-1, that is not targeted by the shRNA. IKD-F11 cells were prepared that stably expressed either GFP, GFP-*Xt*fascin, GFP-*Xt*fascinS33A, or GFP-*Xt*fascinS33D. (The PKC phosphorylation motif is 100% conserved between human and *Xenopus* fascin-1, with the substrate serine at position 33 in *Xenopus*). On a cell population basis, the *Xt*fascin proteins were all expressed at similar levels that represented 35–42% of the content of endogenous fascin (Supplemental Figure 2). On induction of shRNA expression by doxycycline, the endogenous fascin protein level decreased to ~30% of control levels in all lines, whereas the *Xt*fascin proteins remained at 80–85% of their levels in control cells and thus constituted the major form of fascin in the cells (Supplemental Figure 2B). Whereas GFP-, GFP-*Xt*fascin–, or GFP-*Xt*fascinS33A–expressing cells cultured in the absence of doxycycline and

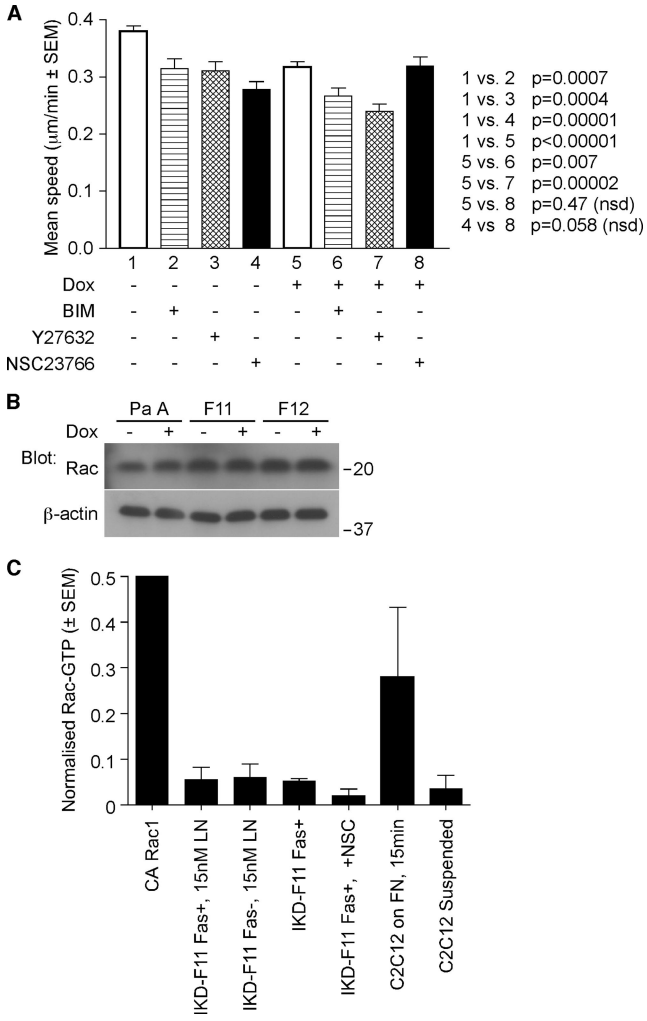

Figure 4. Migration of fascin-knockdown cells is insensitive to Rac inhibition. (A) Migration speeds of IKD-F11 Fas+ cells (lanes 1–4) and IKD-F11 Fas− cells (lanes 5–8) adherent on 15 nM LN were calculated from time-lapse movies under control conditions (1, 4) or after pretreatment with 1 μM BIM (2, 6), 10 μM Y27632 (3, 7), or 100 μM NSC23766 (4, 8). Columns 1 and 4 represent the mean of nine independent experiments; other columns are means of three experiments. Bars indicate SEM, and p values are shown on the figure. See also Supplemental Movies 5 and 6. (B) Rac immunoblot to show that Rac protein levels were unchanged upon fascin depletion. Cell lysates were prepared from cells adhered to 15 nM LN for 2 h. (C) Rac activity is equivalent in LN-adherent IKD-F11 Fas+ and Fas− cells. Controls were constitutively active (CA) Rac1 protein and C2C12 cells in suspension or adhered to 50 nM FN for 15 min. Each column represents the mean of three experiments; bars indicate SEM.

then adhered to LN had similar morphologies to each other and to SW480-Pa cells, many of the GFP-*Xt*fascin-S33D–expressing cells were rounded (Figure 5A, top row).

On doxycycline treatment, the protrusions of GFP-expressing cells were noted to be smaller and similar to those of IKD-F11 Fas− cells (Figure 5A, middle row). GFP-*Xt*fascin–expressing cells were a mixed population of extended and rounded cells; the extended cells had complex protrusions and filopodia similar to those of SW480-Pa and IKD-F11 Fas+ cells (Figure 5A, middle row). Thus, the phenotype of fascin knockdown was rescued by expression of GFP-*Xt*fascin cDNA. In contrast, GFP-*Xt*fascinS33A–expressing cells in the presence of

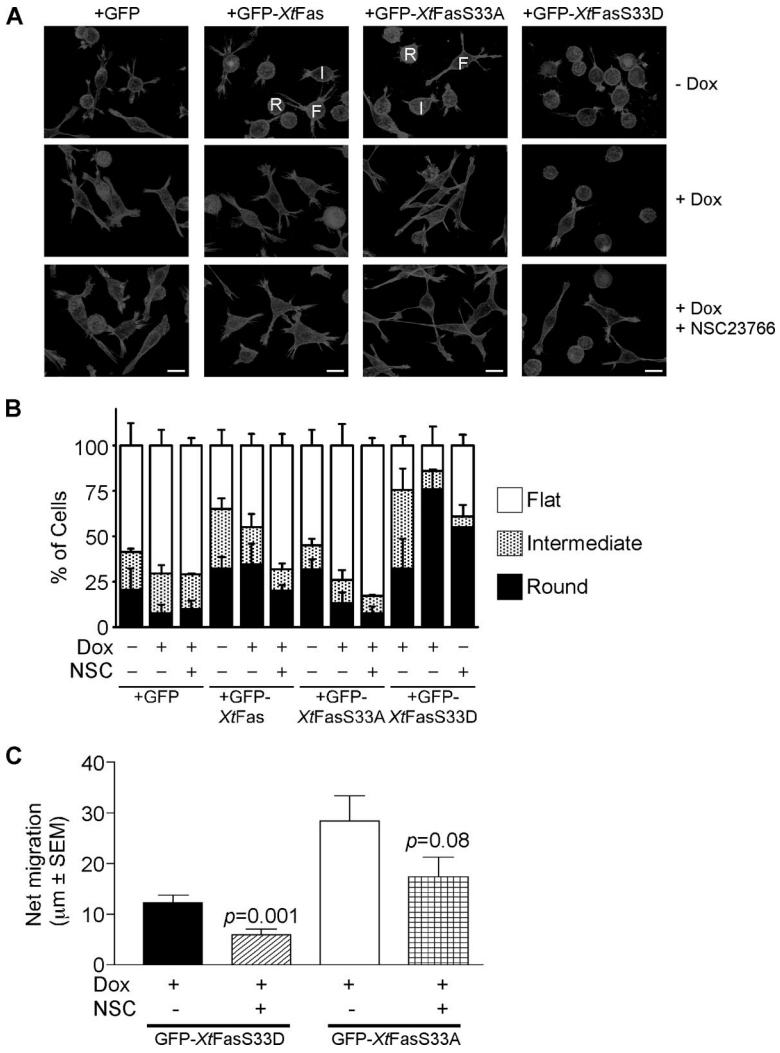

Figure 5. Properties of IKD-F11 cells rescued with wild-type or mutant fascins. (A) F-actin organization in the cell lines under different experimental conditions as indicated. All cells were plated on 15 nM LN for 2 h. NSC23766 treatment was 100 μM for 18 h. Bars, 20 μm. Representative of three independent experiments. (B) quantification of cell morphologies in the absence or presence of rescue with wild-type or mutant fascins. Cell morphologies were scored in three categories: round [R], intermediate [I] and flat [F] (examples of the categories are labeled in A). Each column represents mean data from >100 cells derived from two to four independent experiments; bars indicate SEM. (C) Effect of Rac inhibition on directional persistence of GFP-*Xt*fasS33D and GFP-*Xt*fasS33A cells. The net displacement of cells migrating on 15 nM LN for 200 min, without or with treatment with 100 μm NSC23766, was calculated from time-lapse movies. Each column represents the mean from at least 30 cells, bars indicate SEM. See also Supplemental Movies 7 and 8.

doxycycline were uniformly more extended, with large lobed lamellipodia and fingerlike protrusions. In the presence of doxycycline, most of the GFP-*Xt*fascinS33D–expressing cells were rounded, with small circumferential actin ruffles or blebs. A minority of cells (<20%) had larger actin-containing projections (Figure 5A, middle row). These morphological alterations were confirmed by a quantified analysis in which cells were categorized as flat, intermediate or round (examples of each morphology are labeled in Figure 5A). This scoring demonstrated the extended morphology of GFP-*Xt*fascinS33A–expressing cells in the presence of doxycycline and the contrasting rounded morphology of GFP-*Xt*fascinS33D–expressing cells (Figure 5B).

The distinctive morphologies of cells expressing either GFP-*Xt*fascinS33A or GFP-*Xt*fascinS33D as their major form of fascin suggested that both activities of fascin are normally required for carcinoma cell migration. Indeed, whereas GFP-*Xt*fascin–expressing cells migrated in a similar manner to cells containing endogenous fascin, GFP-*Xt*fascinS33A–expressing cells tended to extend without retraction, forming very long, thin cell protrusions with tiny, dynamic lamellipodia at their tips (Supplemental Movie 7). GFP-*Xt*fascinS33D–expressing cells remained attached and rounded over time, undergoing small, oscillatory movements (Supplemental Movie 8). Kymographic analysis also demonstrated that these cells formed very few membrane extensions (data not shown). In comparison to IKD-F11 Fas+ cells (Figure 3C), the net migration of GFP-*Xt*fascinS33D cells was decreased and that of GFP-*Xt*fascinS33A cells was somewhat increased (Figure 5C). The latter result was probably due to the increased overall length of the cells and their protrusions and did not reach statistical significance versus IKD-F11 Fas+ cells.

To investigate the requirement for active Rac in both activities of fascin, we examined the effect of pre-treatment with NSC23766 on GFP-*Xt*fascinS33A or GFP-*Xt*fascin-S33D cells. Under these conditions, GFP-*Xt*fascin-S33A cells became even more extended and the actin organization in protrusive tips resembled that of IKD-F11 Fas+ cells. The majority of GFP-*Xt*fascinS33D cells remained round (Figure 5A, bottom row). The residual net motility of both cell types was inhibited by NSC23766 (Figure 5C). Thus, both the actin-bundling and PKC-binding activities of fascin are on Rac-dependent pathways.

Wild-Type Fascin Contributes to Tumor Development and Metastasis

To investigate whether depletion of fascin alters tumor cell behavior in vivo, we compared the growth of subcutaneous xenografts of SW480-Pa and IKD-F11 cells in nude mice, in the absence or presence of doxycycline delivered in the

Table 3. Effect of fascin depletion on the development of primary and metastatic xenograft tumors in nude mice

a. Mean tumor volume at day 32

	Tumor volume (mm^3) ± SEM
Pa −Dox (n = 4)	1030.4 ± 506.2
Pa +Dox (n = 4)	1151.9 ± 331.7
F11 −Dox (n = 4)	1181.3 ± 873.7
F11 +Dox (n = 4)	227.7 ± 186.4

b. Incidence of primary and metastatic tumors from SW480Pa and F11 cells

	% Spleen tumor (n)	% Metastasis (n)
Pa −Dox (n = 5)	80.0 (4/5)	100 (5/5)
Pa +Dox (n = 3)	66.7 (2/3)	100 (3/3)
F11 −Dox (n = 4)	100 (4/4)	100 (4/4)
F11 +Dox (n = 6)	16.7 (1/6)	50.0 (3/6)

c. Incidence of primary and metastatic tumors from GFP- or *Xt*Fascin-rescued F11 cells

	% Spleen tumor (n)	% Metastasis (n)
GFP (n = 6)	16.7 (1/6)	0 (0/6)
WT (n = 6)	50.0 (3/6)	33.3 (2/6)
S33A (n = 6)	33.3 (2/6)	16.7 (1/6)
S33D (n = 6)	33.3 (2/6)	0 (0/6)

Experimental conditions and analyses were as described in *Materials and Methods*. In a and b, the indicated groups of mice were given 2 mg/ml doxycycline in the drinking water; in c, all mice were given doxycycline.

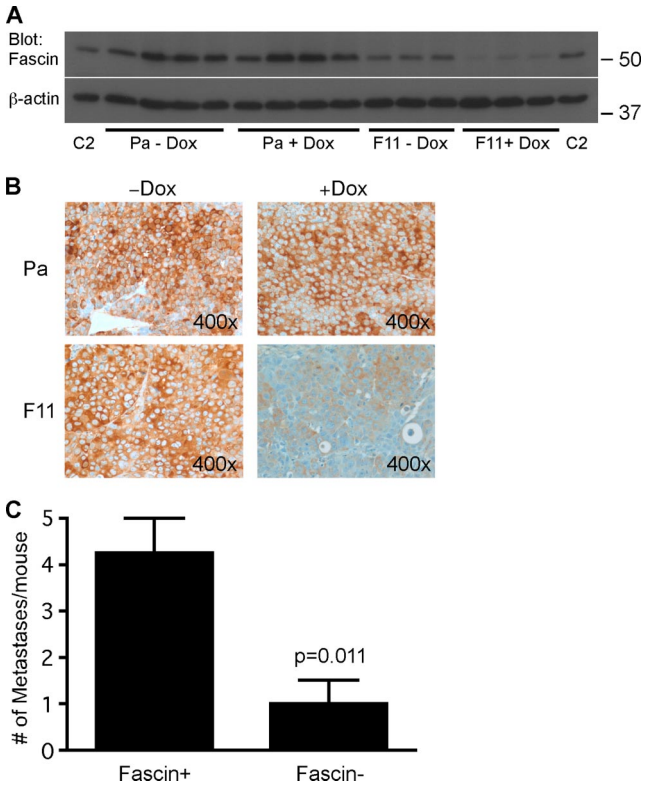

Figure 6. Fascin depletion decreases xenograft tumor development and metastasis in nude mice. (A) Immunoblot for fascin demonstrates that fascin protein levels in the subcutaneous tumors of nude mice given doxycycline in their drinking water were specifically reduced in the mice inoculated with IKD-F11 cells (F11+ Dox). Each lane represents the extract of a single tumor harvested after 32 d; three or four samples are shown for each experimental condition. Extracts of C2C12 cells (C2) were included as positive controls. (B) Immunohistochemical staining for human fascin demonstrates the specific and uniform depletion of fascin protein within the IKD-F11 tumors of nude mice given doxycycline. (C) Metastatic potential of IKD-F11 cells is reduced in nude mice given doxycycline (Fas− condition). Each column represents the mean of at least 6 mice; bars indicate SEM.

drinking water. Whereas the growth of SW480-Pa tumors was not altered in the presence of doxycycline, the development of IKD-F11 tumors was strongly reduced in the presence of doxycycline, such that tumors had only reached a small volume after 32 d (Table 3a). Immunoblot analysis of tumor extracts demonstrated that fascin was effectively and specifically knocked down in the IKD-F11 tumors of mice that had received doxycycline (Figure 6A). Immunohistochemical staining confirmed that fascin protein was uniformly decreased throughout these tumors (Figure 6B). To examine the influence of fascin on metastatic capacity, we compared the development of liver and abdominal metastases from intrasplenically injected SW480Pa or IKD-F11 cells, in nude mice provided without or with doxycycline in their drinking water. The incidence of primary spleen tumors and metastatic tumors was specifically decreased for IKD-F11 cells in the doxycycline-treated mice (Table 3b) and the number of metastatic tumors per mouse was also significantly decreased (Figure 6C).

To compare the activity of fascin point mutants with wild-type fascin, we examined the metastastic capacity of the IKD-F11 cells stably expressing GFP or the wild-type or mutant GFP-*Xt*fascins, as characterized in Figure 5. In this experiment, all mice were treated with doxycycline to deplete the endogenous human fascin of IKD-F11 cells. Whereas cells expressing GFP-*Xt*fascin showed a clear increase in primary tumor growth and metastasis compared with cells expressing GFP only, cells expressing either GFP-*Xt*fascinS33A or GFP-*Xt*fascinS33D had only a small enhancement of primary tumor growth and minimal metastatic capacity (Table 3c). These findings demonstrate that the actin-bundling and PKC-binding activities of fascin are both needed for metastasis in vivo as they are for carcinoma migration in vitro.

DISCUSSION

Fascin expression correlates with poor prognosis in multiple forms of human carcinoma, but its functional role has been unclear. Previous in vitro studies documented effects of fascin on carcinoma cell migration, but the underlying processes have not been defined (Jawhari *et al*., 2003; Hashimoto *et al*., 2005b; Xie *et al*., 2005). Through shRNA depletion of fascin in colon carcinoma cells, and rescue with wild-type and mutant cDNAs, we have established that fascin contributes to the migration of human colon carcinoma cells in vitro and tumor development and metastasis in vivo. Mechanistically, we demonstrate that 1) fascin makes multiple specific contributions to carcinoma migration by impacting on the assembly of filopodia and associated protrusions and the

disassembly of focal adhesions, 2) Rac acts as an upstream regulator of the activities of fascin in cell migration, and 3) both the actin-bundling and active PKC-binding activities of fascin are needed for fascin to promote tumor metastasis.

The observation that fascin-depletion leads to a stronger phenotype in transfilter chemotactic migration than in haptokinetic migration (Figure 3) is consistent with the hypothesis that fascin is required in localized spatial signaling for filopodia formation and directional migration. Previous experiments placed Rac as an upstream regulator of fascin-containing protrusions in skeletal myoblasts, but these experiments focused on the endpoint of lamellipodial assembly; also the active PKC-binding activity of fascin was not appreciated at this time (Adams and Schwartz, 2000). Rac is a well-established regulator of actin polymerization, and, via its substrate p21-activated kinase, activates Lim kinase to inactivate cofilin (Machesky and Hall, 1997; Hartwig *et al*., 1995; Yang *et al*., 1998). These mechanisms impact on the availability of F-actin, which is a prerequisite for F-actin bundling by fascin. More recent studies of normal skeletal myoblasts uncovered that phosphorylated fascin interacts with active PKCα (Anilkumar *et al*., 2003). We demonstrate here that residual net migration in fascin-knockdown cells specifically rescued by expression of a phosphomimetic fascin mutant, GFP-*Xt*fascinS33D, remained susceptible to Rac inhibition. This finding points to unsuspected complexity in the mechanisms by which Rac regulates fascin. The Rac pathway may be particularly suitable as a target to block fascin-dependent cell migration, because it regulates both activities of fascin.

Tractional forces exerted by integrin-based focal adhesions on the local ECM environment are important for the development of lamellipodial protrusions (Wang *et al*., 2001; Parker *et al*., 2002). At the molecular level, substratum adhesion is required for coupling of Rac to its effector p21-activated kinase, and, in cells lacking the focal adhesion protein vinculin, constitutively active Rac is not sufficient to rescue lamellipodia formation (del Pozo *et al*., 2000; Goldmann and Ingber, 2002). We uncovered here that fascin depletion resulted not only in alterations to cell protrusions and loss of filopodia but also in a slower rate of disassembly of focal adhesions. Fascin does not localize to focal adhesions; therefore, we propose that the slower disassembly of focal adhesions upon depletion of fascin is secondarily linked to the loss of filopodia through effects on the actin network in lamellipodia. It is well known that dynamic focal adhesion assembly and disassembly are needed for migration (Webb *et al*., 2003).

The complex phenotype of fascin-depleted cells suggests that coupling between focal adhesions and protrusions is a two-way process. Indeed, several molecular processes including the balance between Rac and Rho activities and microtubule targeting coordinately regulate protrusions and focal adhesions (Sander *et al*., 1999; Wittmann *et al*., 2003; Goldberg and Kloog, 2006). Although we did not observe alterations of the cell body actin cytoskeleton upon fascin depletion, effects on focal adhesions and thereby cell migration could also be a consequence of a lack of competition between fascin and tropomyosin for binding to contractile actomysin filaments (Ishikawa *et al*.,1998). It is highly likely that disruption of a key intracellular mechanical link would alter the forces exerted on focal adhesions by the actin cytoskeleton.

As discussed above, our data establish that reduced assembly of filopodia and protrusions, decreased focal adhesion disassembly, and decreased directional cell migration are all consequences of the acute depletion of fascin. The specificity of these effects was established by normalization of phenotype upon cDNA-based expression of GFP-*Xt*fascin in the knockdown cells (Figure 5). Furthermore, the strikingly different morphologies and migration behavior of cells reconstituted with either nonPKC-binding (GFP-*Xt*fasS33A) or nonactin-bundling (GFP-*Xt*fasS33D) fascin mutants clearly define that both forms of fascin are needed for its function in carcinoma cell protrusions and migration. Our novel data also indicate complexity in the underlying mechanisms: both the phosphorylated and nonphosphorylated forms of fascin act in Rac-dependent pathways.

Importantly, the xenograft tumor experiments revealed that fascin contributes both in the development of primary tumors and in their metastatic spread. The apparent discrepancy between the lack of effect of fascin-depletion on anchorage-independent growth and the clear effect on primary tumor development is not surprising in view that anchorage-independent growth is a good, but not perfect, model for tumorigenicity. In the context of a tumor, stromal-derived or vascular-derived factors provide additional contributions to regulate tumor cell proliferation, tumor vascularization, and the expansion and growth of the tumor. The in vitro anchorage independence colony growth assay does not recapitulate these features. Differing results for soft agar growth and tumor development in vivo have previously been reported for certain oncogenes (e.g., Kim *et al*., 2006). Thrombospondin-1 and -2 do not affect anchorage-independent growth yet strongly inhibit tumor development due to their antiangiogenic activities (Streit *et al*., 1999a,b).

We suggest that the reduced development of primary tumors by fascin-depleted cells could result from a reduced ability of the tumor to expand because of the reduced migratory capacity of the cells. Cell migration is of established significance in metastasis, and we demonstrated here that fascin-depleted cells gave rise to fewer metastases. In accordance with the cell culture migration data, neither GFP-*Xt*fasS33D nor GFP-*Xt*fasS33A fascin mutants rescued metastastic behavior of fascin-depleted cells to the extent that wild-type GFP-*Xt*fascin did. These data demonstrate the biological relevance of the mechanisms identified in cell culture and provide a rationale for considering fascin as a potential therapeutic target as well as a carcinoma biomarker. Putting together our findings with the previously published clinical correlations, the basis for the correlation between high fascin expression and poor prognosis of human carcinomas resides in a contribution of fascin in one or more steps of metastasis. Metastasis is a complex, multistage process in which cell migration is involved at many steps and different steps present greater or lesser obstacles to tumor cell dissemination (Steeg, 2006). It will be of future importance to identify the exact steps at which phosphorylated and nonphosphorylated fascin contributes to metastasis.

ACKNOWLEDGMENTS

We thank Benjamin Tear and Bhavin Patel for assistance with analysis of movies during student projects; Amber Bentley for technical assistance; Becky Haney and Daniel Linder of the CCF Animal Tumor for assistance with the mouse tumor experiments; and the staff of the CCF Flow Cytometry, Imaging, and Molecular Biotechnology core facilities for scientific support. We gratefully acknowledge funding support from the Association for International Cancer Research (grant 04-330 to J.C.A.) and the Royal Society University Research fellowship (to M.P.).

REFERENCES

Adams, J. C. (1997). Characterization of cell-matrix adhesion requirements for the formation of fascin microspikes. Mol. Biol. Cell *8*, 2345–2363.

Adams, J. C. (2004). Roles of fascin in cell adhesion and motility. Curr. Opin. Cell Biol. *16*, 590–596.

Adams, J. C., Clelland, J. D., Collett, G. D., Matsumura, F., Yamashiro, S., and Zhang, L. (1999). Cell-matrix adhesions differentially regulate fascin phosphorylation. Mol. Biol. Cell *10*, 4177–4190.

Adams, J. C., and Schwartz, M. A. (2000). Stimulation of fascin spikes by thrombospondin-1 is mediated by the GTPases Rac and Cdc42. J. Cell Biol. *150*, 807–822.

Akiyama, S. K., Yamada, S. S., Chen, W. T., and Yamada, K. M. (1989). Analysis of fibronectin receptor function with monoclonal antibodies: roles in cell adhesion, migration, matrix assembly, and cytoskeletal organization. J. Cell Biol. *109*, 863–875.

Anilkumar, N., Annis, D. A., Mosher, D. F., and Adams, J. C. (2002). Trimeric assembly of the C-terminal region of thrombospondin-1 or thrombospondin-2 is necessary for cell spreading and fascin spike organisation. J. Cell Sci. *115*, 2357–2366.

Anilkumar, N., Parsons, M., Monk, R., Ng, T., and Adams, J. C. (2003). Interaction of fascin and protein kinase Calpha: a novel intersection in cell adhesion and motility. EMBO J. *22*, 5390–5402.

Carragher, N. O., and Frame, M. C. (2004). Focal adhesion and actin dynamics: a place where kinases and proteases meet to promote invasion. Trends Cell Biol. *14*, 241–249.

Christofori, G. (2006). New signals from the invasive front. Nature *441*, 444–450.

Cohan, C. S., Welnhofer, E. A., Zhao, L., Matsumura, F., and Yamashiro, S. (2001). Role of the actin bundling protein fascin in growth cone morphogenesis: localization in filopodia and lamellipodia. Cell Motil. Cytoskeleton *48*, 109–120.

Condeelis, J., Singer, R. H., and Segall, J. E. (2005). The great escape: when cancer cells hijack the genes for chemotaxis and motility. Annu. Rev. Cell. Dev. Biol. *21*, 695–718.

Costantini, R. M., Falcioni, R., Battista, R., Zupi, G., Kennel, S. J., Colasante, A., Venturo, I., Curcio, C. G., and Sacchi, A. (1990). Integrin ($\alpha 6/\beta 4$) expression in human lung cancer as monitored by specific monoclonal antibodies. Cancer Res. *50*, 6107–6112.

del Pozo, M. A., Price, L. S., Alderson, N. B., Ren, X. D., and Schwartz, M. A. (2000). Adhesion to the extracellular matrix regulates the coupling of the small GTPase Rac to its effector PAK. EMBO J. *19*, 2008–2014.

Friedl, P., and Wolf, K. (2003). Tumour-cell invasion and migration: diversity and escape mechanisms. Nat. Rev. Cancer *3*, 362–374.

Gao, Y., Dickerson, J. B., Guo, F., Zheng, J., and Zheng, Y. (2004). Rational design and characterization of a Rac GTPase-specific small molecule inhibitor. Proc. Natl. Acad. Sci. USA *101*, 7618–7623.

Gilchrist, M. J., Zorn, A. M., Voigt, J., Smith, J. C., Papalopulu, N., and Amaya, E. (2004). Defining a large set of full-length clones from a *Xenopus* tropicalis EST project. Dev. Biol. *271*, 498–516.

Goldberg, L., and Kloog, Y. (2006). A Ras inhibitor tilts the balance between Rac and Rho and blocks phosphatidylinositol 3-kinase-dependent glioblastoma cell migration. Cancer Res. *66*, 11709–11717.

Goldmann, W. H., and Ingber, D. E. (2002). Intact vinculin protein is required for control of cell shape, cell mechanics, and rac-dependent lamellipodia formation. Biochem. Biophys. Res. Commun. *290*, 749–755.

Guo, W., and Giancotti, F. G. (2004). Integrin signalling during tumour progression. Nat. Rev. Mol. Cell Biol. *5*, 816–826.

Hartwig, J. H., Bokoch, G. M., Carpenter, C. L., Janmey, P. A., Taylor, A. L., Toker, A., and Stossel, T. P. (1995). Thrombin receptor ligation and activated Rac uncap actin filament barbed ends through phosphoinositide synthesis in permeabilised human platelets. Cell *82*, 643–653.

Hashimoto, Y., Shimada, Y., Kawamura, J., Yamasaki, S., and Imamura, M. (2004). The prognostic relevance of fascin expression in human gastric carcinoma. Oncology *67*, 262–270.

Hashimoto, Y., Skacel, M., and Adams, J. C. (2005a). Roles of fascin in human carcinoma motility and signaling: prospects for a novel biomarker? Int. J. Biochem. Cell Biol. *37*, 1787–1804.

Hashimoto, Y., Ito, T., Inoue, H., Okumura, T., Tanaka, E., Tsunoda, S., Higashiyama, M., Watanabe, G., Imamura, M., and Shimada, Y. (2005b). Prognostic significance of fascin overexpression in human esophageal squamous cell carcinoma. Clin. Cancer Res. *11*, 2597–2605.

Hashimoto, Y., Skacel, M., Lavery, I. C., Mukherjee, A. L., Casey, G., and Adams, J. C. (2006). Prognostic significance of fascin expression in advanced colorectal cancer: an immunohistochemical study of colorectal adenomas and adenocarcinomas. BMC Cancer *6*, 241.

Haviv, L., Brill-Karniely, Y., Mahaffy, R., Backouche, F., Ben-Shaul, A., Pollard, T.D., and Bernheim-Groswasser, A. (2006). Reconstitution of the transition from lamellipodium to filopodium in a membrane-free system. Proc. Natl. Acad. Sci. USA *103*, 4906–4911.

Ishikawa, R., Yamashiro, S., Kohama, K., and Matsumura, F. (1998). Regulation of actin binding and actin bundling activities of fascin by caldesmon coupled with tropomyosin. J. Biol. Chem. *273*, 26991–26997.

Jawhari, A. U., Buda, A., Jenkins, M., Shehzad, K., Sarraf, C., Noda, M., Farthing, M. J., Pignatelli, M., and Adams, J. C. (2003). Fascin, an actin-bundling protein, modulates colonic epithelial cell invasiveness and differentiation in vitro. Am. J. Pathol. *162*, 69–80.

Kim, S. H., Nakagawa, H., Navaraj, A., Naomoto, Y., Klein-Szanto, A. J., Rustgi, A. K., and El-Deiry, W. S. (2006). Tumorigenic conversion of primary human esophageal epithelial cells using oncogene combinations in the absence of exogenous Ras. Cancer Res. *66*, 10415–10424.

Kyriazis, A. P., DiPersio, L., Michael, G. J., Pesce, A. J., and Stinnett, J. D. (1978). Growth patterns and metastatic behavior of human tumors growing in athymic mice. Cancer. Res. *38*, 3186–3190.

Machesky, L. M., and Hall, A. (1997). Role of actin polymerization and adhesion to extracellular matrix in Rac- and Rho-induced cytoskeletal reorganization. J. Cell Biol. *138*, 913–926.

Maitra, A. *et al*. (2002). Immunohistochemical validation of a novel epithelial and a novel stromal marker of pancreatic ductal adenocarcinoma identified by global expression microarrays: sea urchin fascin homolog and heat shock protein 47. Am. J. Clin. Pathol. *118*, 52–59.

Minn, A. J., Gupta, G. P., Siegel, P. M., Bos, P. D., Shu, W., Giri, D. D., Viale, A., Olshen, A. B., Gerald, W. L., and Massague, J. (2005). Genes that mediate breast cancer metastasis to lung. Nature *436*, 518–524.

Ono, S., Yamakita, Y., Yamashiro, S., Matsudaira, P. T., Gnarra, J. R., Obinata, T., and Matsumura, F. (1997). Identification of an actin binding region and a protein kinase C phosphorylation site on human fascin. J. Biol. Chem. *272*, 2527–2533.

Parker, K. K., Brock, A. L., Brangwynne, C., Mannix, R. J., Wang, N., Ostuni, E., Geisse, N. A., Adams, J. C., Whitesides, G. M., and Ingber, D. E. (2002). Directional control of lamellipodia extension by constraining cell shape and orienting cell tractional forces. FASEB J. *16*, 1195–1204.

Pelosi, G. *et al*. (2003). Independent prognostic value of fascin immunoreactivity in stage I nonsmall cell lung cancer. Br. J. Cancer *88*, 537–547.

Puppa, G. *et al*. (2007). Independent prognostic value of fascin immunoreactivity in stage III-IV colonic adenocarcinoma. Br J. Cancer *96*, 1118–1126.

Sander, E. E., ten Klooster, J. P., van Delft, S., van der Kammen, R. A., and Collard, J. G. (1999). Rac downregulates Rho activity: reciprocal balance between both GTPases determines cellular morphology and migratory behavior. J. Cell Biol. *147*, 1009–1022.

Staquet, M. J., Dezutter-Dambuyant, C., Schmitt, D., Amiot, M., Boumsell, L., and Thivolet, J. (1989). A surface glycoprotein complex related to the adhesive receptors of the VLA family, shared by epidermal Langerhans cells and basal keratinocytes. J. Invest. Dermatol. *92*, 739–745.

Steeg, P. S. (2006). Tumor metastasis: mechanistic insights and clinical challenges. Nat. Med. *12*, 895–904.

Streit, M., Velasco, P., Brown, L. F., Skobe, M., Richard, L., Riccardi, L., Lawler, J., and Detmar, M. (1999a). Overexpression of thrombospondin-1 decreases angiogenesis and inhibits the growth of human cutaneous squamous cell carcinoma. Am. J. Pathol. *155*, 441–452.

Streit, M., Riccardi, L., Velasco, P., Brown, L. F., Hawighorst, T., Bornstein, P., and Detmar, M. (1999b). Thrombospondin-2, a potent enogenous inhibitor of tumour growth and angiogenesis. Proc. Natl. Acad. Sci. USA *96*, 14888–14893.

Svitkina, T. M., Bulanova, E. A., Chaga, O. Y., Vignjevic, D. M., Kojima, S., Vasiliev, J. M., and Borisy, G. G. (2003). Mechanism of filopodia initiation by reorganization of a dendritic network. J. Cell Biol. *160*, 409–421.

Tenchini, M. L., Adams , J.C., Gilberty, C., Steel, J., Hudson, D. L., Malcovati, M., and Watt, F. M. (1993). Evidence against a major role for integrins in calcium-dependent intercellular adhesion of epidermal keratinocytes. Cell Adhes. Commun. *1*, 55–66.

van't Veer, L. J. *et al*. (2002). Gene expression profiling predicts clinical outcome of breast cancer. Nature *415*, 530–536.

Vignjevic, D., Yarar, D., Welch, M. D., Peloquin, J., Svitkina, T., and Borisy, G. G. (2003). Formation of filopodia-like bundles in vitro from a dendritic network. J. Cell Biol. *160*, 951–962.

Vignjevic, D., Kojima, S., Aratyn, Y., Danciu, O., Svitkina, T., and Borisy, G. G. (2006). Role of fascin in filopodial protrusion. J. Cell Biol. *174*, 863–875.

Wang, H. B., Dembo, M., Hanks, S. K., and Wang, Y. (2001). Focal adhesion kinase is involved in mechanosensing during fibroblast migration. Proc. Natl. Acad. Sci. USA *98*, 11295–11300.

Webb, D. J., Brown, C. M., and Horwitz, A. F. (2003). Illuminating adhesion complexes in migrating cells: moving toward a bright future. Curr. Opin. Cell Biol. *15*, 614–620.

Wittmann, T., Bokoch, G. M., and Waterman-Storer, C. M. (2003). Regulation of leading edge microtubule and actin dynamics downstream of Rac1. J. Cell Biol. *161*, 845–851.

Wyckoff, J. B., Segall, J. E., and Condeelis, J. S. (2000). The collection of the motile population of cells from a living tumor. Cancer Res. *60*, 5401–5404.

Xie, J. J., Xu, L. Y., Zhang, H. H., Cai, W. J., Mai, R. Q., Xie, Y. M., Yang, Z. M., Niu, Y. D., Shen, Z. Y., and Li, E. M. (2005). Role of fascin in the proliferation and invasiveness of esophageal carcinoma cells. Biochem. Biophys. Res. Commun. *337*, 355–362.

Yamashiro, S., Yamakita, Y., Ono, S., and Matsumura, F. (1998). Fascin, an actin-bundling protein, induces membrane protrusions and increases cell motility of epithelial cells. Mol. Biol. Cell *9*, 993–1006.

Yang, N., Higuchi, O., Ohashi, K., Nagata, K., Wada, A., Kangawa, K., Nishida, E., and Mizuno, K. (1998). Cofilin phosphorylation and LIM-kinase 1 and its role in Rac-mediated actin reorganisation. Nature *393*, 809–812.

Yoder, B. J., Tso, E., Skacel, M., Pettay, J., Tarr, S., Budd, T., Tubbs, R. R., Adams, J. C., and Hicks, D. G. (2005). The expression of fascin, an actin-bundling motility protein, correlates with hormone receptor-negative breast cancer and a more aggressive clinical course. Clin. Cancer Res. *11*, 186–192.

Zigeuner, R., Droschl, N., Tauber, V., Rehak, P., and Langner, C. (2006). Biologic significance of fascin expression in clear cell renal cell carcinoma: systematic analysis of primary and metastatic tumor tissues using a tissue microarray technique. Urology *68*, 518–522.